PNAS

Supplementary Information for

Exploring switch II pocket conformation of KRAS(G12D) with mutant-selective monobody inhibitors

Padma Akkapeddi[a,1], Takamitsu Hattori[a,b,1], Imran Khan[c,d,1], Eliezra Glasser[a,16], Akiko Koide[s,e], Gayatri Ketavarapu[a], Michael Whaby[c,d], Mariyam Zuberi[c,d], Kai Wen Teng[a], Julia Lefler[f], Lorenzo Maso[a], Injin Bang[a], Michael C. Ostrowski[f], John P. O'Bryan[c,d,2] and Shohei Koide[a,b,2]

[a]Laura and Isaac Perlmutter Cancer Center, New York University Langone Health, New York, NY 10016.
[b]Department of Biochemistry and Molecular Pharmacology, New York University School of Medicine, New York, NY 10016.
[c]Department of Cell and Molecular Pharmacology and Experimental Therapeutics, Hollings Cancer Center, Medical University of South Carolina, Charleston, SC 29425.
[d]Ralph H. Johnson VA Medical Center, Charleston, SC 29425.
[e]Department of Medicine, New York University School of Medicine, New York, NY 10016.
[f]Department of Biochemistry and Molecular Biology, Hollings Cancer Center, Medical University of South Carolina, Charleston, SC 29425.
[1]These authors contributed equally to this work

[2]Correspondence to: Shohei Koide (Shohei.Koide@nyulangone.org) and John P. O'Bryan (obryanjo@musc.edu)

Content

Methods

Protein expression and purification. All proteins used for monobody development and binding assays, including RAS constructs (KRAS4B residues 1–174 containing G12C, G12V, G12D, G13D, WT and monobodies), were produced with an N-terminal tag containing His6, Avi-tag for biotinylation and a TEV protease recognition site using the pHBT vector. The RAS constructs were constructed by Kunkel mutagenesis using a vector encoding the wild-type RAS as the template (1). Monobody genes were amplified from yeast cells and cloned into the pHBT vector (2). The proteins were produced in *E. coli* BL21 (DE3). To produce biotinylated proteins, *E. coli* BL21(DE3) with the pBirA plasmid was used as the host and grown in the presence of 50 μM of biotin. Expressed proteins were purified using Ni-Sepharose columns (Cytiva) via gravitational flow, followed by dialysis in Tris-buffered saline (TBS, 50 mM Tris-Cl pH 7.5 containing 150 mM NaCl) for non-RAS proteins. TBS containing 20 mM $MgCl_2$ and 0.5 mM DTT was used for RAS proteins. Samples were further purified using a Superdex 75 size exclusion column on an AKTA Pure system (Cytiva). The Cys-light version (C51S;C80L;C118S) (3) of KRAS(G12D) (residues 1–169) and monobodies used for crystallization and BLI were produced with the pHBT vector in *E. coli* BL21(DE3) as described above. Following Ni-Sepharose purification, the N-terminal His_6 and Avi tags were removed with TEV protease in the presence of 0.5 mM EDTA and 0.5 mM DTT during overnight dialysis against TEV cleavage buffer (50 mM Tris-Cl pH 8, 50 mM NaCl, 5 mM β-mercaptoethanol, supplemented with 20 mM $MgCl_2$ for KRAS). Cleaved tags and TEV proteases were removed by Ni-Sepharose, followed by size-exclusion chromatography.

Nucleotide exchange of RAS. Purified RAS proteins used in binding experiments and crystallization were prepared by diluting stock protein (typically containing 20–250 μM RAS) 25 times with 20 mM Tris-Cl buffer pH 7.5 containing 5 mM EDTA, 0.1 mM DTT, and 1 mM final concentration of a nucleotide (GDP or GTPγS). Samples were incubated at 30 °C for 30 min. $MgCl_2$ was then added to the sample at a final concentration of 20 mM and the solution was further incubated on ice for at least 5 minutes prior to use.

Monobody development. General procedures for the development of monobodies against purified protein targets have been described previously (1, 4). After four rounds of phage display library selection using biotinylated KRAS(G12D) at concentrations of 100, 100, 50, and 20 nM, the genes encoding monobodies from the enriched phage pool were transferred to a yeast display vector, which was used to construct yeast-display libraries. The yeast display libraries were sorted using a S3e fluorescence-activated cell sorter (Bio-Rad). The first round of sorting recovered clones that bound to KRAS(G12D); the second round recovered clones that did not bind to KRAS(WT); and the third round recovered clones that bound to KRAS(G12D). Single clones were then screened for selective binding to RAS mutants. The expression of monobodies on the surface of yeast cells was detected using mouse anti-V5 (ThermoFisher, MA5-15253, 1:75 for sorting approximately 10^7 yeast cells, and 1:300 for staining 10^5 yeast cells for analysis) followed by labeling using anti-mouse IgG-FITC conjugate (Millipore Sigma, F0257, 1:100). Target binding was detected with

NeutrAvidin Dylight650 (Invitrogen). Yeast cells were analyzed using an iQue flow cytometer (Sartorius). The median of the signal intensity in the Dylight650 channel for the 75–95th percentile population was taken as a representative signal. This sampling method of flow cytometry events minimizes erroneous contributions from events with anomalously high signals while retaining events with high signals.

Biolayer interferometry (BLI) analysis. BLI experiments were performed on an Octet Red96e instrument (Sartorius). Biotinylated KRAS proteins bound to nucleotide were immobilized on streptavidin biosensor tips. Samples were diluted in 20 mM HEPES-NaOH buffer (pH 7.4) containing 150 mM NaCl, 5 mM $MgCl_2$, 0.2 mM TCEP and 0.005% Tween-20. BLI signals were analyzed using Octet Data Analysis software (Sartorius).

Crystallization and X-ray structure determination. Purified and tag-cleaved Cys-light KRAS(G12D) bound to GTPγS or GDP was incubated with purified, tag-cleaved monobody 12D1(K63S) or 12D5(K63S) at a 1:1.1 molar ratio. The K63S mutation was introduced to facilitate crystallization (5). The complexes were purified with a Superdex 75 10/300 SEC column (Cytiva) in 10 mM NaCl, 10 mM Tris-Cl pH8, 20 mM $MgCl_2$ and concentrated to approximately 10 mg/ml. The 12D1(K63S)-KRAS(G12D)•GTPγS complex was crystallized in 2.8 M sodium acetate trihydrate at pH 7.0 when mixed 1:1 in a total volume of 2 μl using a sitting drop vapor diffusion method. The 12D5(K63S)-KRAS(G12D)•GTPγS complex was crystalized in 0.2 M sodium sulfate decahydrate containing 20% w/v PEG 3350 and 0.05% w/v benzamidine hydrochloride when mixed 1:1 in a total volume of 2 μl using a sitting drop vapor diffusion method. Crystals were preserved in the reservoir solution with an additional 20% (v/v) glucose. X-ray diffraction data were collected at the Advance Photon Source at the Argonne National Laboratory using beam line 19-ID. Diffraction data were processed using HKL3000 and HKL2000 (6, 7). The starting models were built by molecular replacement using PDB entries 5VPZ, 5VP7 and 7L0G as search models using Phaser (8). Structural refinement was performed iteratively by using phenix.refine (9), Coot (10) and PDBredo (11). Protein-protein interaction interfaces were analyzed by using PDBePISA server (http://www.ebi.ac.uk/msd-srv/prot_int/pistart.html) (12). The root-mean-square deviations (RSMDs) were calculated by using the Structure Pairwise Alignment Tool available at the RCSB PDB (https://www.rcsb.org/alignment).

Deep mutational scanning. A yeast-display library of 12D4 was constructed by changing residues V27, T28, V29, V30, F31, D33, E47, T49, S51, G52, S53, K75, Y76, L77, F78, W79, S80, G81 and Y82 to all 20 amino acids, one amino acid at a time. Oligonucleotides including the NNK codon, where N is a mixture of A, T, G and C and K is a mixture of G and T, for the intended randomized position were used to introduce the mutations using PCR. Three separate reactions were performed with pooled oligonucleotides for closely located positions: sub-library 1 for V27, T28, V29, V30, F31 and D33; sub-library 2 for E47, T49, S51, G52 and S53; and sub-library 3 for K75, Y76, L77, F78, W79, S80, G81 and Y82. Yeast display vectors encoding the full-length monobody genes containing mutations fused with aga2 gene and V5 tag were constructed

using yeast homologous recombination. Next, the yeast cells containing the combined library were incubated with either biotinylated KRAS G12D complexed with GTPγS or GDP, either 10 nM or 100 nM, as well as anti-V5 antibody, using the conditions described in the monobody development section above, and the binding and non-binding populations were sorted. Plasmids encoding the monobody genes were purified using Zymoprep Yeast Plasmid Miniprep II (Zymo Research Corporation, D2004), and the monobody genes were amplified using primers that are designed for amplicon sequencing with different index sequences. The PCR products were sequenced using MiSeq (Illumina). Sequencing data were analyzed using a set of UNIX and Python scripts developed in house to deduce the number of reads for each mutation.

Cell culture. Cell lines (HEK293T, HPAF-II) used in the study were directly purchased from ATCC, H358 was validated externally via IDEXX (H358), Panc-1 cells were previously validated by STR analysis (13). Pa14C and PSN1 cells were the kind gifts of Dr. Aaron Hobbs and were previously validated by STTR analysis. HEK293T, Panc-1 and HPAF-II cells were maintained in DMEM high glucose with L-glutamine (Hyclone) supplemented with 10% FBS (Gemini Bio-products) and antibiotics-antimycotics (Gibco). H358 cells were maintained in RPMI-1640 high glucose with sodium pyruvate, L-glutamine (Thermo), supplemented with 10% FBS and penicillin/streptomycin. The absence of mycoplasma contamination was periodically confirmed using a PCR-based mycoplasma testing kit (eMyco, Bulldog Bio). Pa14C and PSN1 cells were grown in RPMI with 10% FBS. All culture media were purchased commercially (Corning). Transient transfection in HEK-293, HEK-293T and NIH/3T3 cells was done using polyethyleneimine (PEI). For HEK-293 and HEK-293T, typically, 3 μl of 1 mg/ml PEI stock was used for each μg of DNA in Opti-MEM reduced serum media (Life Technologies). Opti-MEM-PEI mixture was incubated for 10 minutes at room temperature. Next, DNA was added to Opti-MEM: PEI cocktail and incubated for at least 20 minutes at room temperature. The Opti-MEM: PEI-DNA mixture was added to cells in serum-free media and incubated for three hours after which the media was replaced with fresh complete media. Transfections in NIH/3T3 cells were done with the same procedures, however, 5 μl of 1 mg/ml PEI stock was used for each μg of DNA.

Colocalization assays. HEK293T cells were cultured in glass-bottom 8-well chambers (ibidi GmbH) for colocalization assays for 1 day prior to transfection. On the day of transfection at 70–90% confluency, media were replaced with antibiotics-free complete media (DMEM supplemented with 10% FBS). The vectors encoding mCherry-fused monobodies were constructed by cloning their genes into the pEGFP vector at the NheI and ApaI restriction enzyme sites. The pEGFP KRAS4B vector was a gift of Prof. Mark Philips. Transfection of HEK293T cells with pEGFP vectors encoding the appropriate mCherry fused monobodies and EGFP fused KRAS4B constructs was performed with lipofectamine 3000 (Thermo Fisher Scientific) and according to the manufacturer's recommended protocol. On the following day, transfected cells were imaged with a LSM710 confocal microscope (Zeiss).

Pull-down assays. HPAF-II, Panc1 and H358 cells were cultured in 10 cm plates (Corning, #430167). Cells were lysed by incubating them on ice for 15 min in GTPase lysis buffer (25 mM Tris-Cl pH 7.2, 150 mM NaCl, 5 mM $MgCl_2$, 1% NP-40, and 5% glycerol supplemented with protease inhibitor tablet (Roche, 5892991001) and phosphatase inhibitors (1 mM sodium orthovanadate, 10 mM NAF, 54 mM β-glycerol phosphate)) immediately before analysis. After centrifugation for 15 min at 15,000 × g, the supernatants were collected and incubated with SA agarose resins (Thermo Fisher Scientific) for 1h at 4 °C to remove molecules that nonspecifically bound to the resins. After the removal of the resins via centrifugation, the precleared lysates were then incubated with biotinylated monobodies or the RAS-Binding domain (RBD) of RAF bound to SA agarose resins for 3 hr at 4 °C while rotating. The agarose resins were then washed twice with the GTPase lysis buffer and boiled in 1x SDS buffer with 37.5 mM β-mercaptoethanol and processed for western blotting. RAS proteins were detected using a mouse pan-RAS antibody (SCBT, sc-166691, 1:500) followed by anti-mouse HRP conjugate (Pierce, 31432, 1:4000) with the ECL 2 Western blotting substrate (Pierce; 80196).

Generation of stably transduced, monobody-expressing PDAC cells. HEK293T cells were used to generate viral particles for DOX-inducible 12D4 expression. The packaging HEK293T cells were transfected by calcium phosphate using pCW57.1-CFP-12D4 (transfer plasmid) along with a plasmid encoding packaging plasmid (pCMVdR8.74) and the viral envelope (pMD2.G) in 4:3:1 ratio to generate viral particles. On the following day, packaging cells were placed in fresh media and on day 2 post-transfection, conditioned media cells were collected, filtered, and used to infect PDAC cells followed by selection in tetracycline-free media containing puromycin (1-2 μg/ml). Following selection, colonies were pooled to generate a polyclonal cell line that was used for all subsequent analyses.

Immunoblotting and antibodies. Cell lysates were made by washing cells once in cold PBS followed by lysis in PLC buffer (50 mM HEPES, pH 7.5, 150 mM NaCl, 10% glycerol, 1% Triton X-100, 1 mM EGTA, 1.5 mM magnesium chloride, 100 mM sodium fluoride supplemented with 1 mM vanadate, 10 μg/ml leupeptin and 10 μg/ml aprotinin). For making tumor lysates, tumors were harvested and transferred to round-bottomed microfuge tubes and snap-frozen by immersing in liquid nitrogen. 40-50 mg of the tissue was homogenized using an electric homogenizer in about 1 ml of cold PLC buffer on ice. Homogenized tissue was passed through a 70 μm cell strainer to clear the lysates and centrifuged at 13,000 rpm for 20 minutes at 4 °C. The supernatant was collected and transferred to fresh tubes. The lysates were directly used for protein estimation and analysis or stored at -80 °C for later use. For cell lysates, 5-10 mg of the whole cell lysates (WCL) were used to detect FLAG tagged monobody, HA tagged RAS, ERK or pERK by western blotting. For tumor lysates, 15-20 mg of the lysates were used. The following antibodies were used: monoclonal anti-HA (clone 16B12, Biolegend #90154), polyclonal rabbit anti-HA (Poly9023, Biolegend #923502), monoclonal anti-FLAG (Clone M2, Sigma #F1804), polyclonal rabbit anti-FLAG

(Sigma #F7425), anti-phospho-ERK (Thr202/Tyr204, CST #9101), anti-ERK (CST #9102), anti-vinculin (SC #73614).

Co-immunoprecipitation and signaling assays. HEK293 cells were transfected with the indicated constructs. Following immunoprecipitation of CFP-FLAG-Mb using FLAG antibody, samples were analyzed by Western blot for co-precipitation of the HA-tagged RAS. For transient cell signaling assays, HEK293 cells were transfected with indicated HA-tagged RAS mutant constructs or FLAG-tagged CFP-Mb or FLAG-tagged CFP alone and analyzed for effects on MAPK signaling as previously described (13). For analysis of signaling in RAS mutant tumor cell lines, cells were treated with 2-4 μg/ml of DOX for 48 hours, serum starved overnight then lysed in buffer and analyzed as described previously (13) using phosphospecific ERK (pERK) or total ERK antibodies.

NIH/3T3 transformation assay. Freshly revived NIH/3T3 cells were seeded in 60 mm dishes to a density of 2.5×10^5 cells in complete media. Cells were transfected with the indicated constructs and media changes were performed every 2 days. Foci were stained with 0.1% crystal violet and counted after 15 days for KRAS(G12D) transfectants and 21 days for KRAS(G13D) transfectants. All assays were performed in triplicate.

Soft agar colony formation assay. Soft agar colony formation assays were performed essentially as described previously (13). Cells were fed 1–2x per week with media with or without 2-4 μg/ml doxycycline (DOX) to induce expression of Mb. Two to three weeks after plating, cells were stained using MTT (100 μl of 2 mg/ml per well). Colony numbers and average colony size were quantified using ImageJ.

Mouse xenograft tumor assay. For the xenograft tumor assays, five-week-old male or female athymic nude mice were purchased from Charles River Laboratories (CRL) and acclimatized for one week. A 100 μl suspension of 10×10^6 cells in a 1:1 solution (v/v) of serum-free RPMI/Matrigel basement membrane matrix was injected subcutaneously (s.c) into the flanks of mice. Two days following injection, mice were randomly assigned to control (-DOX) or treatment (+DOX) cohorts. Cells were assessed for their ability to form tumors in the absence (-DOX) or presence of Mb expression (+DOX). DOX was provided at 2 mg/ml in water supplemented with sucrose. All animal experiments described herein were in compliance with protocols approved by the Institutional Animal Care and Use Committees at the Medical University of South Carolina and the Ralph H Johnson VA Medical Center.

Flow cytometric analysis of tumor samples. Tumor samples were dissociated using the Miltenyi gentleMACS tumor dissociation kit (130-096-730). Briefly, tumors were dissected and cut into small pieces using a razor blade. The samples were then added to gentleMACS C tubes (130-090-753) and placed on a Miltenyi gentleMACS Octo with heaters (130-096-427). The gentleMACs program 37m-TDK-2 was used

to dissociate the tumors. After dissociation, each sample was filtered through 70 μm and then 100 μm membrane. After centrifugation, cells were suspended in FACS buffer (PBS containing 0.1% BSA) and washed twice. The Zombie Aqua Fixable Viability Kit (Biolegend #423101) was used before cells were fixed and permeabilized using the eBioscience Foxp3/Transcription Factor Staining Buffer set (#00-5523). Cells were then incubated with fluorescent dye-conjugated Cleaved-Caspase 3 (CST #9661; 1:50) and Ki-67 (Abcam #16667; 1:200) antibodies for 30 minutes at room temperature. Cells were washed twice and resuspended in FACS buffer for flow analysis. Samples were analyzed on a BD FACS Verse and analyzed with FlowJo software (BD Life Sciences).

Statistical analysis. The statistical methods are described either in figure legends, figures, and results sections throughout the main text. The data (bar graphs), unless otherwise specified, are presented as mean ± standard deviation. In xenograft mice experiments, “N” represents the number of animals utilized in each treatment group. The investigators were blinded during evaluation of tumor size variations following treatments and staining analysis for flow cytometry. All statistical analysis was performed using GraphPad Prism v9 software for Mac. Significance between two groups was assessed by the Student’s two-tailed t test.

References

1. Teng KW*, et al.* (2021) Selective and noncovalent targeting of RAS mutants for inhibition and degradation. *Nat Commun* 12:2656.
2. Sha F*, et al.* (2013) Dissection of the BCR-ABL signaling network using highly specific monobody inhibitors to the SHP2 SH2 domains. *Proc Natl Acad Sci U S A* 110:14924-14929.
3. Ostrem JM, Peters U, Sos ML, Wells JA, & Shokat KM (2013) K-Ras(G12C) inhibitors allosterically control GTP affinity and effector interactions. *Nature* 503:548-551.
4. Koide A, Wojcik J, Gilbreth RN, Hoey RJ, & Koide S (2012) Teaching an Old Scaffold New Tricks: Monobodies Constructed Using Alternative Surfaces of the FN3 Scaffold. *J Mol Biol* 415:393-405.
5. Wojcik J*, et al.* (2010) A potent and highly specific FN3 monobody inhibitor of the Abl SH2 domain. *Nat Struct Mol Biol* 17:519-527.
6. Minor W, Cymborowski M, Otwinowski Z, & Chruszcz M (2006) HKL-3000: the integration of data reduction and structure solution--from diffraction images to an initial model in minutes. *Acta Crystallogr D Biol Crystallogr* 62:859-866.
7. Otwinowski Z & Minor W (1997) Processing of X-ray diffraction data collected in oscillation mode. *Methods Enzymol* 276:307-326.
8. McCoy AJ*, et al.* (2007) Phaser crystallographic software. *J Appl Crystallogr* 40:658-674.
9. Afonine PV*, et al.* (2012) Towards automated crystallographic structure refinement with phenix.refine. *Acta Crystallogr D Biol Crystallogr* 68:352-367.
10. Emsley P, Lohkamp B, Scott WG, & Cowtan K (2010) Features and development of Coot. *Acta Crystallogr D Biol Crystallogr* 66:486-501.
11. Joosten RP, Long F, Murshudov GN, & Perrakis A (2014) The PDB_REDO server for macromolecular structure model optimization. *IUCrJ* 1:213-220.
12. Krissinel E & Henrick K (2007) Inference of macromolecular assemblies from crystalline state. *J Mol Biol* 372:774-797.
13. Khan I*, et al.* (2022) Identification of the nucleotide-free state as a therapeutic vulnerability for inhibition of selected oncogenic RAS mutants. *Cell Rep* 38:110322.

Supplementary Table 1. X-ray diffraction data collection and refinement statistics

	12D1-KRAS (G12D) (8EZG)	12D5-KRAS (G12D) (8F0M)
Data collection		
Space group	*P 64 2 2*	*P 21 2 21*
Cell dimensions		
a, *b*, *c* (Å)	156.48, 156.48, 64.62	151.39, 44.73, 88.16
α, β, γ (°)	90, 90, 120	90, 90, 90
Resolution (Å)	50-2.52 (2.56-2.52)[a]	50-2.44 (2.48-2.44)[a]
R_{merge}	0.092 (0.324)	0.091 (0.308)
R_{pim}	0.033 (0.113)	0.061 (0.207)
$CC_{1/2}$	0.986 (0.973)	0.939 (0.905)
CC*	0.996 (0.993)	0.984 (0.975)
$I / \sigma I$	20.3 (7.4)	12.4 (5.0)
Completeness (%)	99.9 (99.9)	98.4 (99.7)
Redundancy	8.7 (9.0)	3.3 (3.2)
Refinement		
Resolution (Å)	45.17-2.52	42.90-2.44
No. reflections	16,122	23,331
R_{work} / R_{free}	0.171/0.213	0.201/0.245
No. atoms		
Protein	2034	4019
Ligand/ion	30	86
Water	144	102
B-factors		
Protein	48.43	48.88
Ligand/ion	33.51	50.81
Water	46.41	41.25
R.m.s. deviations		
Bond lengths (Å)	0.008	0.005
Bond angles (°)	1.26	1.05
Ramachandran favored (%)	98.43	97.60
Ramachandran allowed (%)	1.57	2.20
Ramachandran outliers (%)	0.00	0.20
Clashscore	4.66	5.31
Interface area ($Å^2$)[b]		
Monobody-KRAS(G12D)	914.4	946.2 (GTPγS) 942.9 (GDP)

[a]Values in parentheses are for highest-resolution shell. [b]Interface area calculation was performed using PDBePISA server (http://www.ebi.ac.uk/msd-srv/prot_int/pistart.html).

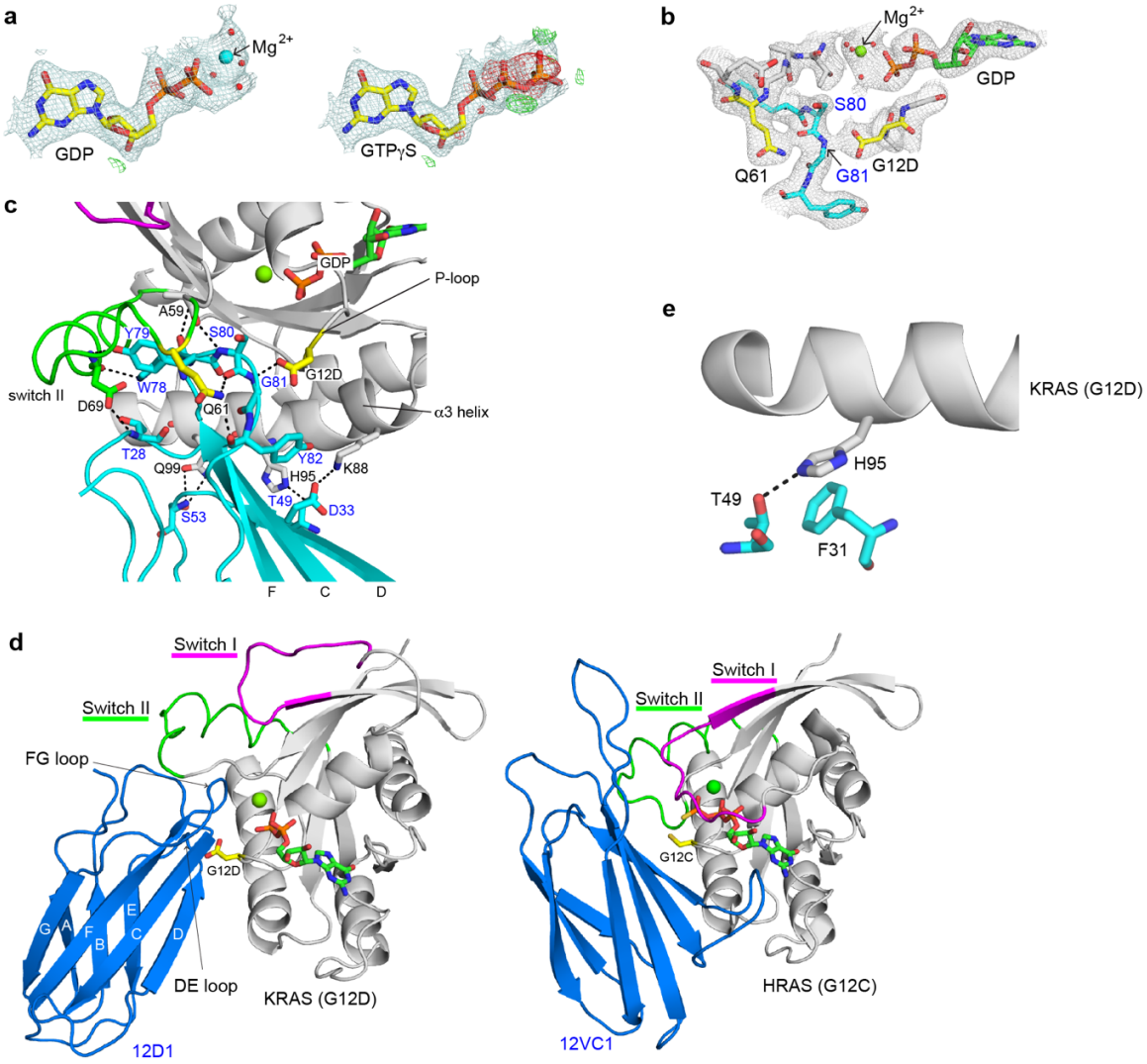

Supplementary Figure 1. Crystal structure of 12D1(K63S) in complex with KRAS(G12D)•GDP, related to Figure 2. (**a**) Results of interpreting the electron density map of the region surrounding the bound nucleotide as GDP (left) and GTPγS (right). The 2mFo-DFc map contoured at 1 σ (light cyan mesh) and mFo-DFc map with negative (red mesh) and positive (green mesh) density contoured at 3 σ are shown. The conformation of GDP and the Mg^{2+} coordination are consistent with other KRAS(G12D)•GDP structures, and no negative density was found in this region (left). Negative density around β- and γ-phosphate of GTPγS was observed for GTPγS (right), and the conformation of GTPγS differs from that of GTP analogs in other KRAS(G12D) structures (see also Supplementary Figure 4b). These observations justify our interpretation of the electron density as GDP instead of GTPγS. (**b**) The 2mFo-DFc composite omit map (contoured at 1 σ) of the binding interface around G12D (yellow) and Q61 (yellow) of KRAS(G12D) (gray). The residues of monobody 12D1(K63S) are shown in cyan. The water molecules (except for those coordinating with Mg^{2+}) are omitted for clarity. (**c**) Details of the interaction interface between 12D1(K63S) and KRAS(G12D). The color scheme is the same as in Figure 2b. The C, D and F strands of 12D1 are

labeled. The dashed lines indicate hydrogen bonds. (**d**) Structural comparison of the 12D1(K63S)-KRAS(G12D)•GDP complex (left panel) with the 12VC1-HRAS(G12C)•GTPγS complex (PDB: 7L0G, right panel). Monobodies are shown in blue and the RAS proteins are shown in gray. G12D and G12C are shown in the stick model in yellow. The beta-strands and the DE and FG loops of 12D1 are labeled. (d) A close-up view of the interaction between $H95^{RAS}$ and $F31^{Mb}$ and $T49^{Mb}$. The dashed line indicates a hydrogen bond.

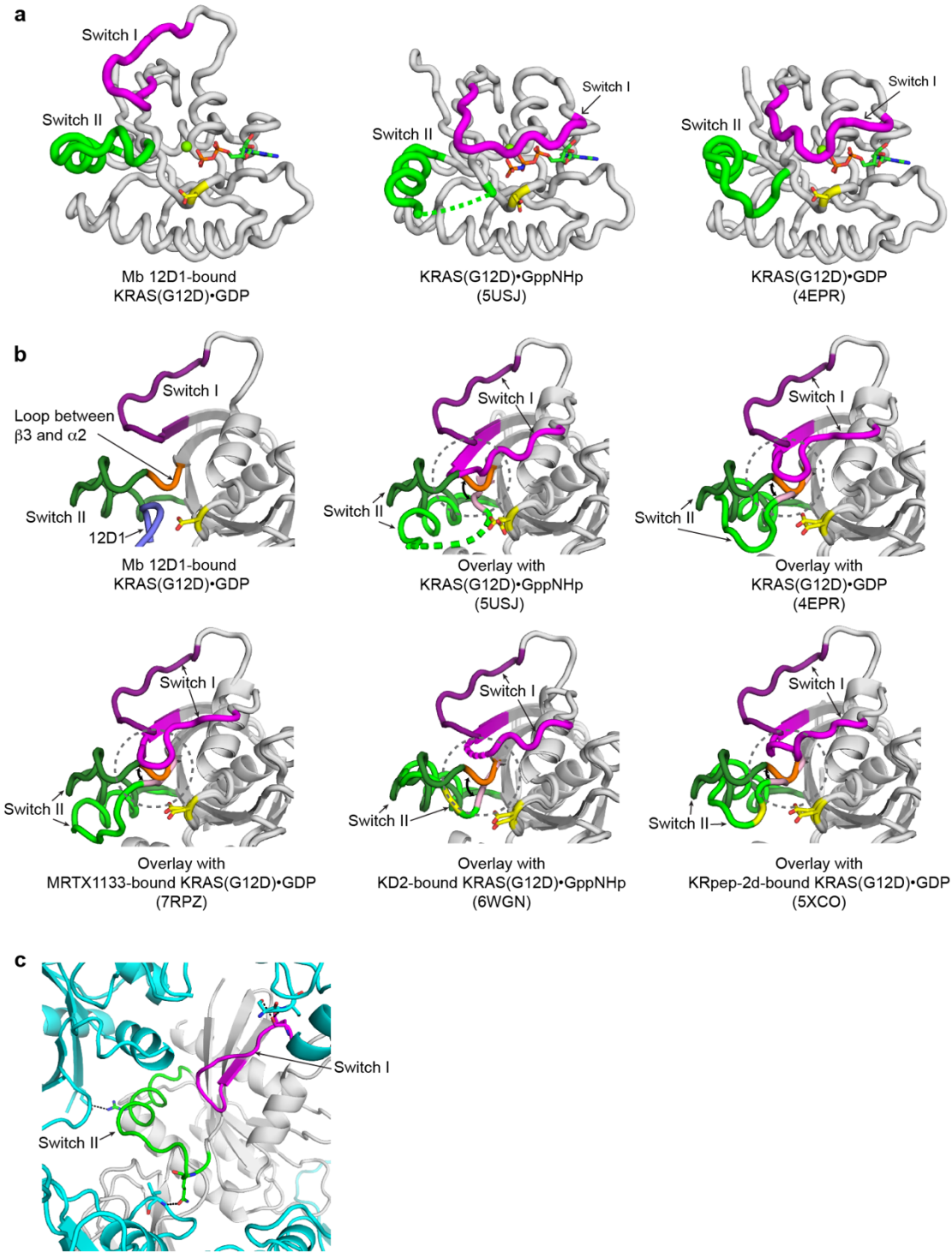

Supplementary Figure 2. Comparisons of the conformations of the switch I and switch II regions of KRAS. (**a**) Comparison of 12D1(K63S)-bound KRAS(G12D)•GDP (left panel) with KRAS(G12D) •GppNHp (PDB: 5USJ, center panel) and KRAS(G12D)•GDP (PDB: 4EPR, right panel). The switch I and switch II regions are shown in magenta and green, respectively. Monobody 12D1(K63S) in the left panel is not shown for clarity. (**b**) Overlay of 12D1(K63S)-bound KRAS(G12D)•GDP (top left) with other KRAS(G12D) structures.

The switch I, switch II regions and the loop region between the β3 strand and the α2 helix in the 12D1(K63S)-bound KRAS(G12D)•GDP complex are shown in dark purple, dark green and orange, respectively. The color scheme for other KRAS(G12D) structures is the same as in (**a**). The loop region followed by the switch II region is shifted toward the switch I region upon binding of monobody 12D1(K63S), which likely causes the conformational shift of the switch I region. Indeed, the switch I region in other KRAS(G12D) structures would cause steric hindrance with the switch II region observed in the 12D1(K63S)-bound KRAS(G12D)•GDP complex, as shown in the overlaid structures. (**c**) Crystal packing near the switch I and switch II regions of the KRAS(G12D)•GDP in complex with 12D1(K63S). The proteins in the asymmetric unit (ASU) and the symmetric unit are shown in gray and cyan, respectively. The switch I and switch II regions in the complex in the ASU are shown in magenta and green, respectively. The dashed lines indicate polar interactions.

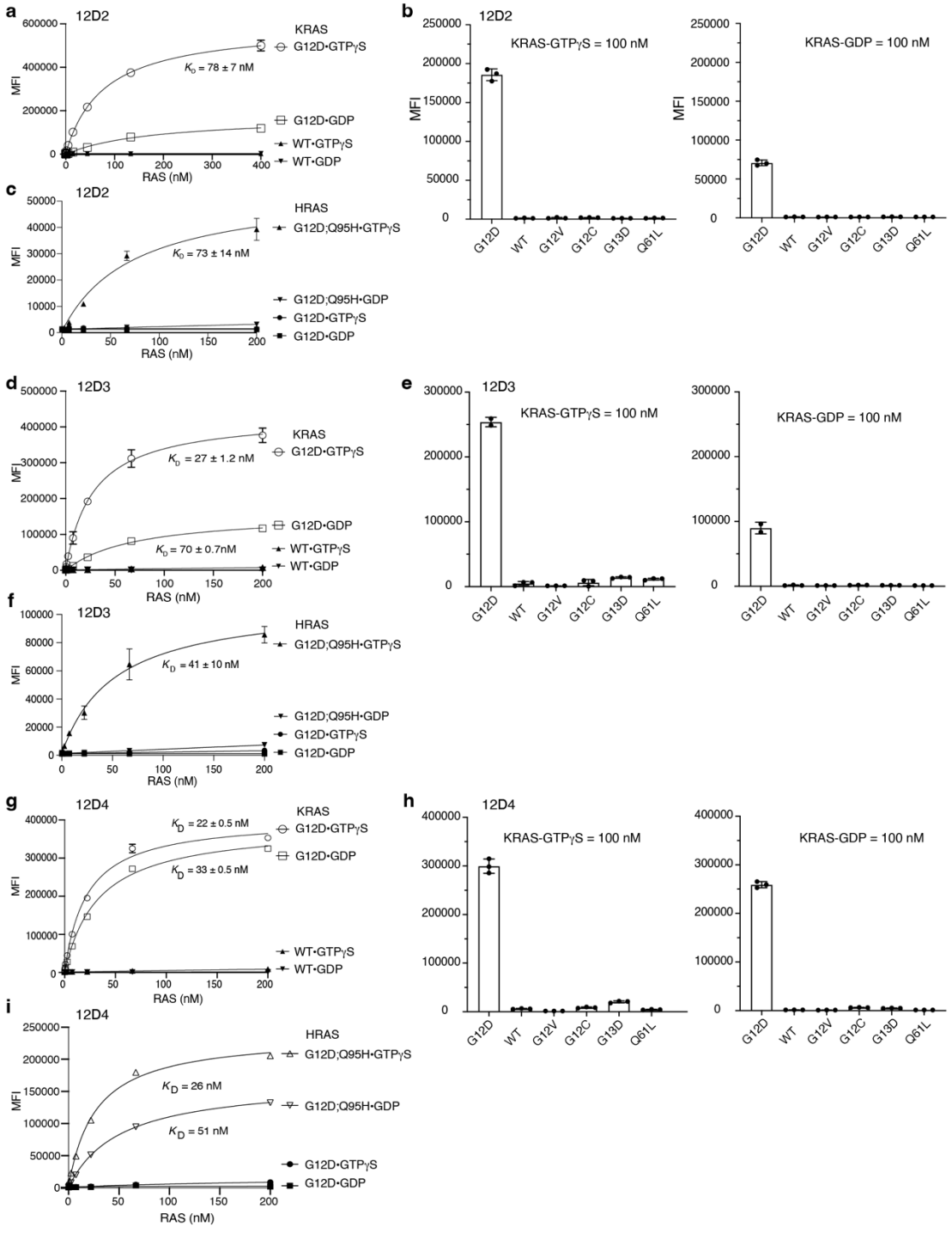

Supplementary Figure 3. Yeast display characterization of KRAS(G12D)-selective monobodies, 12D2, 12D3 and 12D4. (**a**) Binding titrations of KRAS(G12D) and KRAS(WT) to yeast cells displaying the 12D2 monobody. (**b**) Specificity of 12D2 to different KRAS mutants in the GTPγS- and GDP-bound states. (**c**) Binding titrations of HRAS(G12D) and HRAS(G12D:Q95H) to yeast cells displaying 12D2. (**d**) Binding titrations of KRAS(G12D) and KRAS(WT) to yeast cells displaying the 12D3 monobody. (**e**) Specificity of

12D3 to different KRAS mutants in the GTPγS- and GDP-bound states. (**f**) Binding titrations of HRAS(G12D) and HRAS(G12D:Q95H) to yeast cells displaying 12D3. (**g**) Binding titrations of KRAS(G12D) and KRAS(WT) to yeast cells displaying the 12D4 monobody. (**h**) Specificity of 12D4 to different KRAS mutants in the GTPγS- and GDP-bound states. (**i**) Binding titrations of HRAS(G12D) and HRAS(G12D:Q95H) to yeast cells displaying 12D4. Data shown are the mean and s.d. (n = 3).

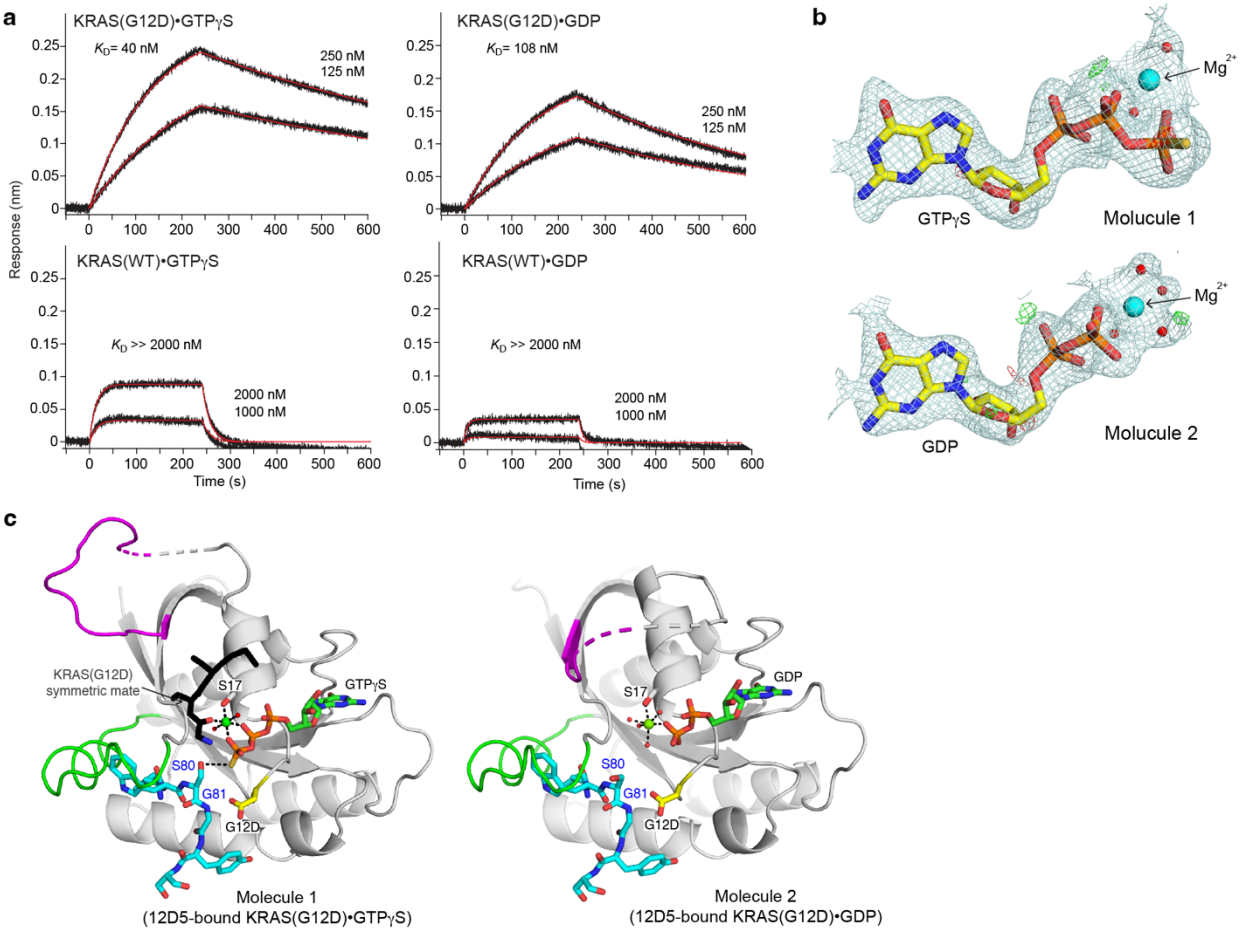

Supplementary Figure 4. Binding characterization of the 12D5 monobody and crystal structures of 12D5 in complex with KRAS(G12D)•GTPγS and with KRAS(G12D)•GDP. (**a**) BLI sensorgrams of the interaction between 12D5 and KRAS. The indicated KRAS proteins were immobilized and the binding of the soluble 12D5 sample was measured. The K_D values are from the global fit of a 1:1 binding model to the data. (**b)** The 2mFo-DFc and mFo-DFc difference maps of the region surrounding the bound nucleotide of two KRAS molecules in the asymmetric unit. The maps are shown in the same manner as Supplementary Fig. 1a. The conformation of nucleotides and Mg^{2+} coordination are consistent with other KRAS(G12D) structures. No negative density was observed in these regions. **c**) The conformations of two KRAS molecules found in the asymmetric unit of 12D5-bound KRAS(G12D). The color scheme is the same as in Figure 2. KRAS is shown as cartoon with the $D12^{RAS}$ side chains and bound nucleotides in stick models. Only the residues of 12D5 monobody surrounding $D12^{RAS}$ are shown in cyan for clarity.

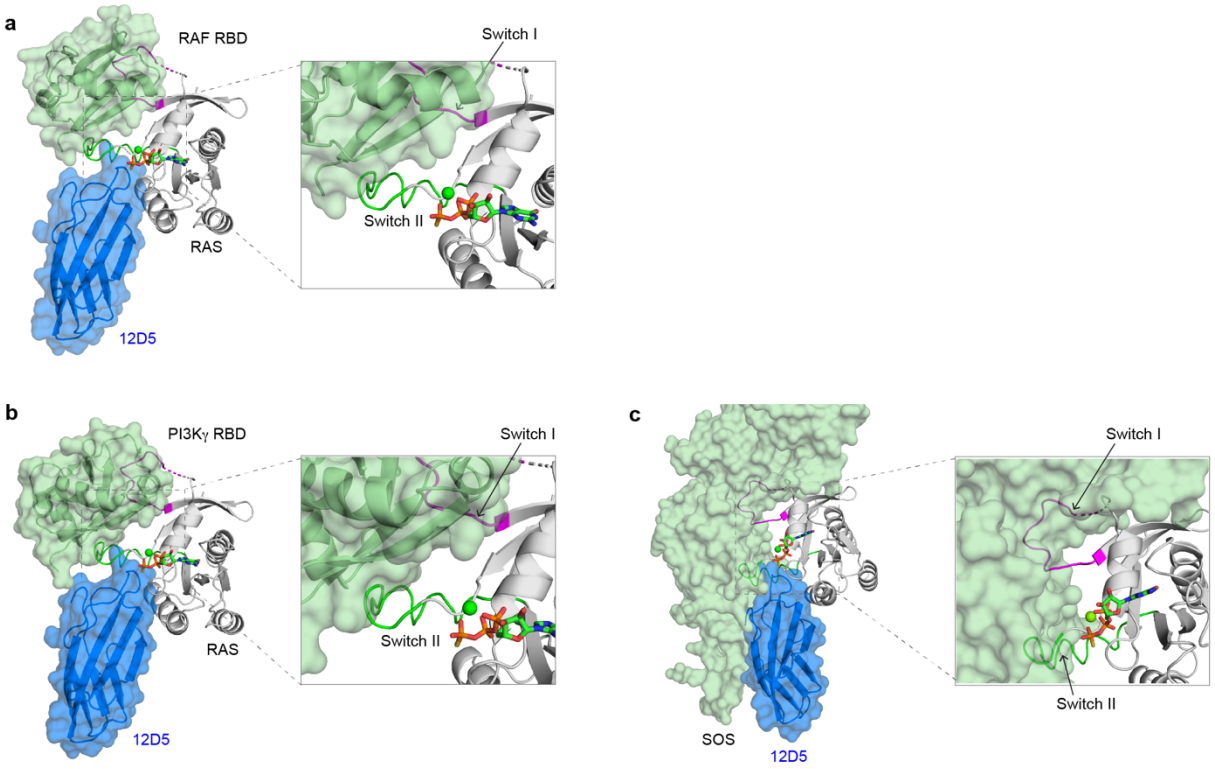

Supplementary Figure 5. Incompatibility of the 12D5-KRAS(G12D)•GTPγS complex with binding to natural RAS-binding partners. (**a**) An overlay of the 12D5-RAS(G12D) complex and a RAF RBD-KRAS(WT) complex (PBD: 6XHB) using the RAS molecules as the references. RAF RBD-bound KRAS(WT) is not shown for clarity. The box shows the steric hindrance between the switch regions of KRAS(G12D) and RAF RBD (green). (**b**) An overlay of the 12D5-RAS complex and an RAS-PIK3γ RBD complex (PBD: 1HE8) in the same manner as in (a). (**c**) An overlay of the 12D5-RAS complex and a SOS-HRAS•GppNHp complex (PDB: 1NVV) in the same manner as in (a). HRAS• GppNHp is not shown for clarity.

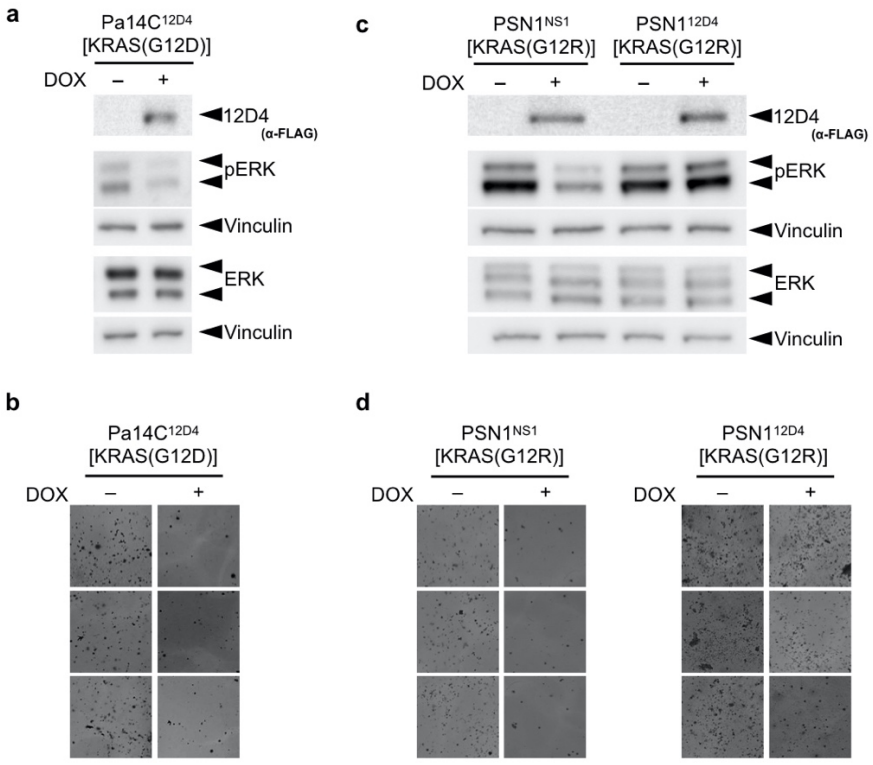

Supplementary Figure 6. Induction of 12D4 expression selectively inhibits signaling and growth of PDAC cells harboring KRAS(G12D)**.** (**a, c**)**.** Doxycycline (DOX) inducible 12D4 expressing stable lines were generated from *RAS* mutant tumor cells. ERK-MAPK activation was then measured with and without DOX treatment by Western blot analysis for pERK levels. The RAS mutant expressed in each tumor line is indicated above the panels. Vinculin expression was used as a control for loading. (**b, d**) Inhibition of anchorage independent growth by intracellular expression of 12D4. The indicated cells engineered to express 12D4 under DOX control were plated on soft agar in the absence (–) or presence (+) of DOX and allowed to grow for 3-4 weeks.12D4 expression inhibited anchorage independent growth only in cells harboring KRAS(G12D). The NS1 monobody, which is mutation-agnostic, was used as a positive control.

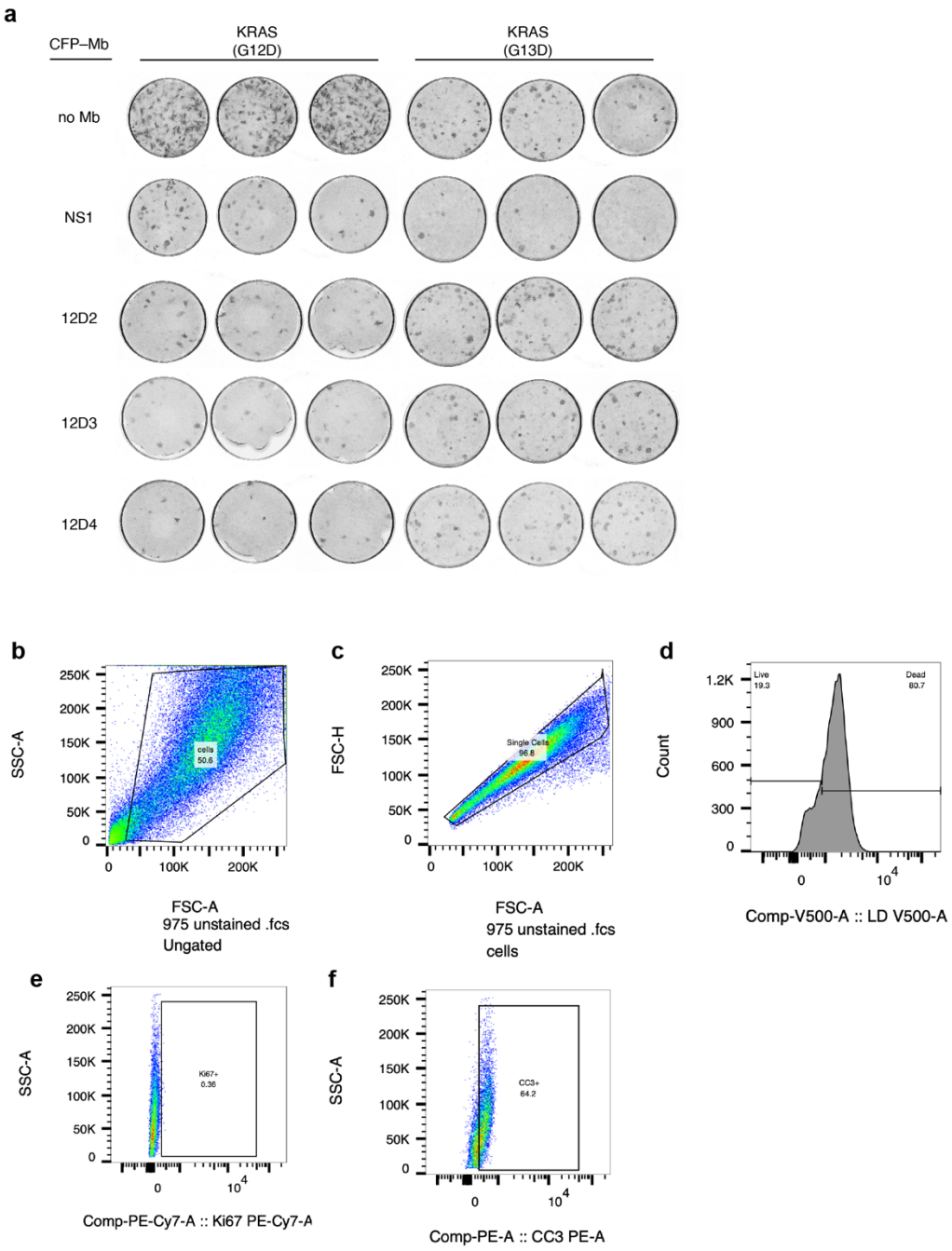

Supplementary Figure 7. (a) Raw data for NIH/3T3 transformation assay shown in Fig. 6g. The cells were transfected with the indicated RAS mutants along with CFP or CFP-tagged monobodies and allowed to grow at confluence for 2-3 weeks. Foci were visualized with crystal violet. (**b-f**) Gating strategy for flow cytometry analysis of tumor samples shown in Figure 7. All cells from the harvested tissue (of mouse and human origins) were analyzed (b). The single-cell population was gated first (b), then the live-cell population was gated (d). All the live cells were analyzed for Ki-67 (e) and CC3 (f). The gating strategy is shown on representative data.